How aortic valve annular plane systolic excursion and left ventricular strains are associated in healthy adults measured simultaneously by three-dimensional speckle-tracking echocardiography? (Insights from MAGYAR-Healthy Study)

Attila Nemes, Nóra Ambrus, Csaba Lengyel

Department of Medicine, Albert Szent-Györgyi Medical School, University of Szeged, Szeged, Hungary

Contributions: (I) Conception and design: A Nemes; (II) Administrative support: N Ambrus; (III) Provision of study materials or patients: A Nemes, N Ambrus; (IV) Collection and assembly of data: A Nemes; (V) Data analysis and interpretation: A Nemes, C Lengyel; (VI) Manuscript writing: All authors; (VII) Final approval of manuscript: All authors.

Correspondence to: Attila Nemes, MD, PhD, DSc. Department of Medicine, Albert Szent-Györgyi Medical School, University of Szeged, H-6725 Szeged, Semmelweis Street 8, Hungary. Email: nemes.attila@med.u-szeged.hu.

Background: Aortic valve annular (AVA) plane systolic excursion (AAPSE) is an echocardiographic measure of left ventricular (LV) function, representing the spatial AVA displacement throughout the heart cycle. This study focused on examining associations between AAPSE and LV strains, as objective features of LV contractility patterns, assessed simultaneously by three-dimensional (3D) speckle-tracking echocardiography (3DSTE) in healthy adult individuals. It was also examined what happens when these parameters are at, or smaller or larger than, their mean values.

Methods: The present cohort study consisted of 111 healthy subjects (average age: 35.1±12.3 years, 70 men), In all individuals, two-dimensional Doppler echocardiography and 3DSTE have been utilized, the latter was used for simultaneous assessment of LV strains and AAPSE.

Results: Apical LV longitudinal strain proved to be increased in the presence of lower-than-average AAPSE. Midventricular, apical and global LV circumferential strain proved to be elevated in the presence of higher-than-average AAPSE. AAPSE showed no significant differences when comparing global LV strain subgroups having lower/higher than average and agerage values, but showed the lowest value for the average global LV radial, circumferential and longitudinal strains.

Conclusions: There is a balanced sensitive relationship between AAPSE and regional LV strains as assessed during the same 3DSTE in healthy adults.

Keywords: Annulus; aortic valve (AV); healthy speckle-tracking echocardiography; three-dimensional (3D)

Submitted Nov 19, 2025. Accepted for publication Feb 12, 2026. Published online Feb 27, 2026.
doi: 10.21037/qims-2025-aw-2493
View this article at: https://dx.doi.org/10.21037/qims-2025-aw-2493

Introduction

Aortic valve (AV) annular (AVA) plane systolic excursion (AAPSE) is an echocardiographic measure of left ventricular (LV) systolic performance and longitudinal function, representing the spatial AVA displacement throughout the heart cycle (1-4). Although M-mode echocardiography (MME) offers a simple and feasible way to measure AAPSE (3,4), a more accurate assessment of the three-dimensional (3D) spatial motion of the AVA is now possible with 3D echocardiography (5). This can be done in a way that other features of LV function can be measured simultaneously with AAPSE, including quantitative measures of LV contractility in the 3D space (6,7). This capability allows for the simultaneous examination of physiological parameters such as measurement of AAPSE and LV strains, features of LV contractility, even in healthy subjects in a non-invasive manner, helping to better understand their relationship (6-8). Therefore, this study focused on investigating associations between AAPSE and regional and global LV strains, assessed by 3D speckle-tracking echocardiography (3DSTE) simultaneously in the same healthy adult subjects (9-14). It was also examined what happens when these parameters are at, below, or above their average values. We present this article in accordance with the STROBE reporting checklist (available at https://qims.amegroups.com/article/view/10.21037/qims-2025-aw-2493/rc).

Methods

Subject population

The present cohort study consisted of 111 healthy individuals (mean age: 35.1±12.3 years, 70 men), who were willing to voluntarily participate in this study between 2011 and 2017. All examined parameters were normal, including physical examination, standard 12-lead electrocardiography (ECG), laboratory tests, and two-dimensional (2D) Doppler echocardiography. No one had known disorders or pathological states that could affect findings, were regularly taking any medications, were smokers, were pregnant, athletes, or obese (body mass index >30 kg/m^2). The present study is part of the 'Motion Analysis of the heart and Great vessels bY three-dimensionAl speckle-tRacking echocardiography in Healthy subjects' (MAGYAR-Healthy Study), in which physiologic analyses were performed between 3DSTE-derived variables and other parameters for better understanding cardiac mechanics in healthy individuals ('Magyar' means 'Hungarian' in Hungarian language). This study was conducted in accordance with the Declaration of Helsinki and its subsequent amendments. Institutional and Regional Human Biomedical Research Committee at the University of Szeged, Hungary approved the project (No. 71/2011, latest approval was given on 17th March, 2025). All participants provided written informed consent.

2D echocardiography with Doppler

In all cases, 2D echocardiography was used to determine left atrial and LV sizes, and modified Simpsons' method-derived LV ejection fraction (EF) using a Toshiba Artida® cardiac ultrasound tool (Toshiba Medical Systems, Tokyo, Japan) equipped with a broadband (1–5 MHz) PST-30BT phased-array transducer (15). Doppler echocardiography was utilized for exclusion of significant valvular stenoses or regurgitations, and to determine transmitral diastolic flow velocities [early (E) and late (A)].

3DSTE

The 3DSTE studies were conducted in two stages (9-14). First, 3D echocardiographic datasets were acquired by the Toshiba Artida® echocardiographic tool, but the transducer was switched to a 3D-capable PST-25SX matrix-array probe. Following settings optimizations (magnitude, gain, etc.), acquisition of 3D datasets was performed from the window at LV apex. The subjects were asked to hold their breath for optimal images, at which point at constant RR intervals on ECG six subvolumes over six cardiac cycles were acquired. These echocardiographic datasets were automatically stitched together by the software. The second step was performed at a later date to analyze the acquired datasets using a vendor-provided dedicated software, 3D Wall Motion Tracking version 2.7 (UltraExtend, Toshiba Medical Systems, Tokyo, Japan). At this time LV strains were measured together with determination of AAPSE. Using apical long-axis two-chamber (AP2CH) and four-chamber (AP4CH) views and three cross-sectional views at different levels of the LV, following optimizations, markers were set to the apical LV endocardium and the LV–mitral annulus edges by the observer. Then automatic reconstruction of the LV endocardial surface and creation

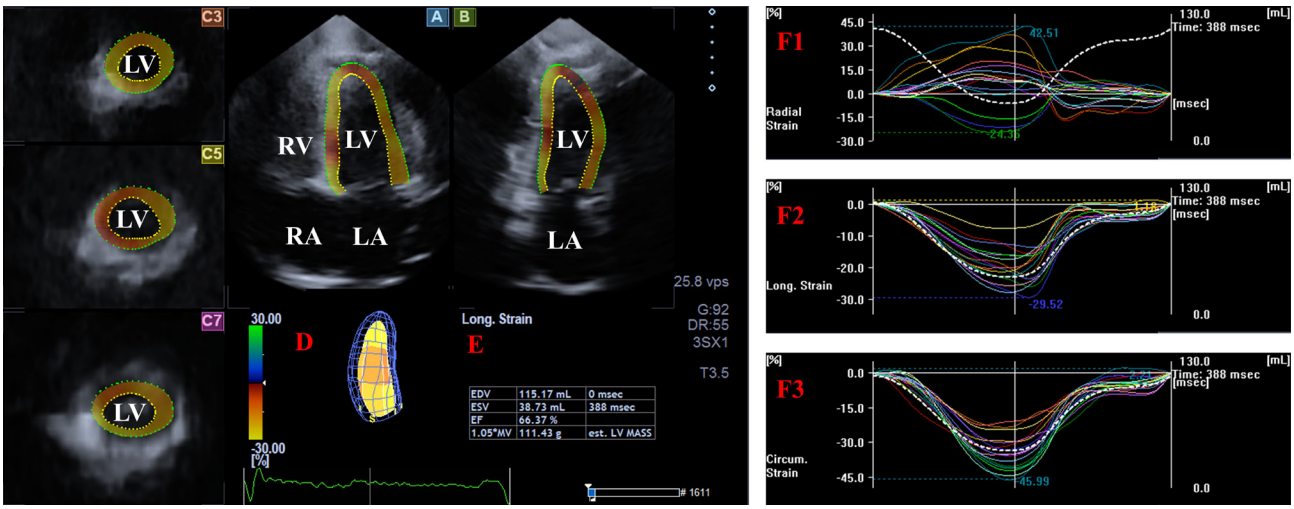

Figure 1 3D speckle-tracking echocardiographic measurement LV strains. Representative apical four-chamber (A) and two-chamber (B) long-axis views are shown alongside apical (C3), midventricular (C5), and basal (C7) short-axis cross-sections, all of which were automatically reconstructed from the 3D echocardiographic dataset. Panel (D) (red) illustrates the 3D model of the LV, while panel (E) (red) displays the corresponding LV volumes and ejection fraction. Time—LV radial, longitudinal, and circumferential global (white) and segmental (coloured) strain curves together with time—LV volume change (dashed white) curve are also presented (F1–F3). 3D, three-dimensional; LA, left atrium; LV, left ventricle; RA, right atrium; RV, right ventricle.

of the 3D virtual cast of the LV was done by the software following sequential analysis. Using this LV model, the following unidimensional/unidirectional LV strains were measured:

- Radial strain (RS) –thinning/thickening of the LV region;
- Longitudinal strain (LS) –shortening/lengthening of the LV region;
- Circumferential strain (CS) –narrowing/widening of the LV region.

Segmental strain assessments were carried out using the 16-segment model of the LV. Moreover, regional, mean segmental and global strains were also measured (9-14) (*Figure 1*).

To determine the position of the AVA, AP4CH and AP2CH long-axis views were used for optimal LV longitudinal planes. After AV/aorta visualization by optimizing and tilting the longitudinal planes, they were positioned to be parallel to the centerline of the aortic root in these views. Alignment of the AVA relied on a C7 cross-sectional view positioned perpendicularly to the longitudinal plane. Precision was maintained by confirming that the C7 remained perpendicular to the centerline and by avoiding any assessments within the sinus of Valsalva or the LV outflow tract. AAPSE was defined as the spatial AVA displacement throughout the heart cycle measured in end-diastole and end-systole (5) (*Figure 2*).

Statistical analysis

Mean ± standard deviation (SD) or counts (percentages) formats were used to present data. Levene's test was used to test homogeneity of variances. To test the normality of distribution, Shapiro–Wilk test was carried out. For datasets exhibiting a normal distribution, independent-samples *t*-tests were employed. In contrast, non-normally distributed data were analyzed using the Mann-Whitney-Wilcoxon test. To account for multiple comparisons, a one-way analysis of variance (ANOVA) supplemented with Bonferroni correction was applied, where necessary. Linear regression analysis was used to assess potential correlations between AAPSE and global LV-LS, LV-RS, and LV-CS. To test reproducibility of 3DSTE-derived AAPSE and LV strain measurements, intra- and interobserver reliability were assessed in a cohort of 30 healthy volunteers, reporting both the mean ± 2SD of differences and intraclass correlation coefficients (ICCs). A P value of less than 0.05 was defined as the threshold for statistical significance.

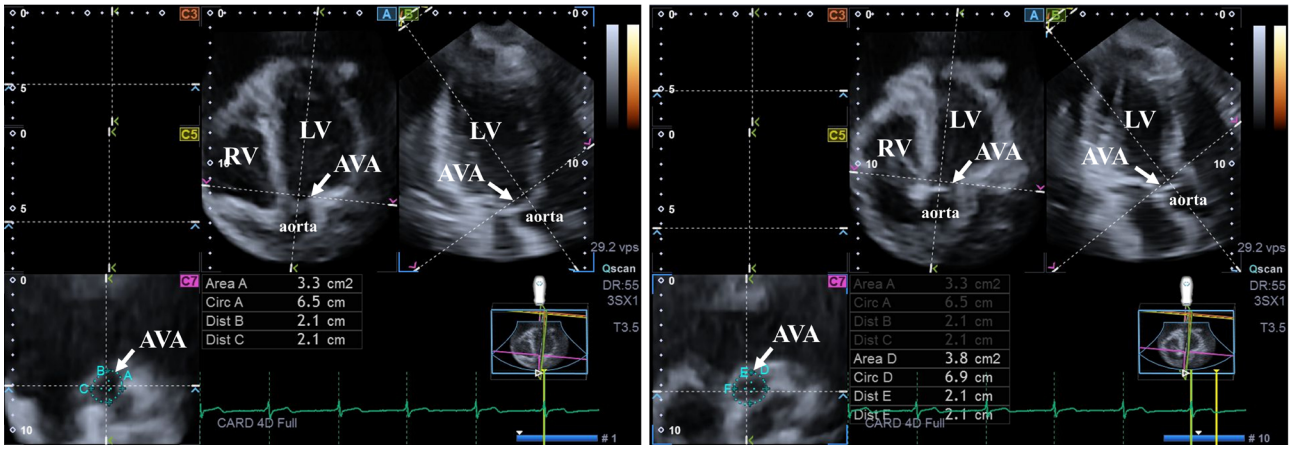

Figure 2 Three-dimensional speckle-tracking echocardiography-derived assessment of the aortic valve annular (AVA) dimensions in end-diastole (left panel) and in end-systole (right panel): apical 4-chamber (A) and 2-chamber (B) long-axis views optimized for the AVA and 'en-face' view of the AVA in C7 cross-sectional view. Area, AVA area; AVA, aortic valve annulus; Circ, AVA perimeter; Dist B, maximum AVA diameter; Dist C, minimum AVA diameter; LV, left ventricle.

Table 1 Clinical and two-dimensional echocardiographic data

Data	Measures
Clinical data	
n	111
Mean age (years)	35.1±12.3
Males [%]	70 [63]
Systolic blood pressure (mmHg)	122±2
Diastolic blood pressure (mmHg)	81±3
Heart rate (bpm)	73±2
Height (cm)	174.0±12.4
Weight (kg)	73.4±15.6
Two-dimensional echocardiographic data	
LA diameter (mm)	37.1±3.6
LV end-diastolic diameter (mm)	48.4±3.4
LV end-systolic diameter (mm)	32.3±3.1
LV end-diastolic volume (mL)	106.9±23.5
LV end-systolic volume (mL)	38.3±9.0
Interventricular septum (mm)	9.2±1.4
LV posterior wall (mm)	9.4±12
LV ejection fraction (%)	64.5±4.1
Early diastolic mitral inflow velocity - E (cm/s)	77.9±16.5
Late diastolic mitral inflow velocity - A (cm/s)	59.3±13.9

Data are presented as mean ± standard deviation. LA, left atrial; LV, left ventricular.

All computational analyses were performed using SPSS software (version 29.0, IBM Corp., Armonk, NY, USA).

Results

Clinical, 2D echocardiographic data with Doppler and 3DSTE data

Data are presented in *Table 1*. No one had valvular regurgitation (larger than or equal to grade 1) or significant stenosis on any valves.

Classification of subjects

Categorization of healthy adults was done based on their average ± SD of 3DSTE-derived AAPSE (1.16±0.30 cm) and global LV-RS (25.5%±9.2%), global LV-CS (27.6%±5.0%) and global LV-LS (–16.1%±2.3%). During analysis, the following cut-off values were used using their mean ± SD:

- For AAPSE: 0.86 and 1.46 cm;
- For global LV-RS: 16.3% and 34.7%;
- For global LV-CS: –22.6% and –32.6%;
- For global LV-LS: –13.8% and –18.4%.

LV strains in different AAPSE subgroups

Apical LV-LS was elevated in the presence of lower-than-average AAPSE. Midventricular, apical and global LV-

Table 2 Aortic valve annular dimensions and systolic excursion of its plane in different aortic valve annular plane systolic excursion groups

Data	AAPSE ≤0.86 cm (n=18)	0.86 cm < AAPSE <1.46 cm (n=75)	1.46 cm ≤ AAPSE (n=18)	ANOVA P value
AAPSE (mm)	0.71±0.09	1.15±0.16†	1.63±0.16†‡	0.01
Basal LV-RS (%)	29.8±9.3	33.3±12.1	32.2±13.6	0.81
Midventricular LV-RS (%)	28.8±9.3	29.9±9.7	29.2±14.3	0.88
Apical LV-RS (%)	17.8±8.6	17.1±8.1	19.8±12.7	0.79
Global LV-RS (%)	24.6±8.0	25.7±8.8	25.4±11.5	0.78
Mean segmental LV-RS (%)	26.4±7.7	28.0±8.2	28.0±11.3	0.87
Basal LV-CS (%)	−25.1±5.1	−26.3±4.6	−25.8±6.0	0.86
Midventricular LV-CS (%)	−30.0±5.1	−29.0±5.2	−31.8±7.3‡	0.85
Apical LV-CS (%)	−34.0±10.1	−29.2±10.2	−34.3±10.8‡	0.89
Global LV-CS (%)	−28.3±4.7	−27.0±4.7	−29.4±5.7‡	0.87
Mean segmental LV-CS (%)	−29.2±4.8	−28.0±4.5	−30.2±5.5	0.86
Basal LV-LS (%)	−18.9±4.3	−20.5±4.3	−20.7±4.8	0.90
Midventricular LV-LS (%)	−13.2±4.7	−13.5±3.5	−13.0±2.4	0.91
Apical LV-LS (%)	−19.7±4.9	−16.1±5.6†	−17.3±4.1	0.78
Global LV-LS (%)	−16.0±2.1	−16.0±2.3	−16.4±2.3	0.92
Mean segmental LV-LS (%)	−17.0±1.9	−16.8±2.2	−17.0±2.3	0.92

Data are presented as mean ± standard deviation. †, P<0.05 *vs.* AAPSE ≤0.86 cm; ‡, P<0.05 *vs.* 0.86 cm < AAPSE <1.46 cm. AAPSE, aortic valve annular plane systolic excursion; CS, circumferential strain; LS, longitudinal strain; LV, left ventricular; RS, radial strain.

CS were increased in the presence of higher-than-average AAPSE (*Table 2*).

AAPSE in different global LV strain subgroups

AAPSE showed no significant differences between global LV strain subgroups, but showed the lowest value for the average global LV-LS, LV-CS and LV-RS. The complex relationships of regional LV strains in different global LV subgroups are also presented (*Tables 3-5*).

Linear regression analysis

Linear regression analysis revealed no significant correlations between AAPSE and global LV-LS (r=0.15, P=0.33), global LV-RS (r=0.14, P=0.35) or global LV-CS (r=0.32, P=0.31).

Reproducibility of AAPSE and LV strains

Reproducibility parameters for AAPSE and global LV strains are presented in *Table 6*.

Discussion

One consequence of technological advances in cardiovascular imaging in recent decades is that it is now possible to perform assessments that can provide answers to certain (patho)physiological phenomena that are difficult to study. Moreover, all of this can be done non-invasively, as many times as needed, using virtual, easy-to-create models in 3D even in healthy individuals. Echocardiography has been the basis of cardiovascular imaging for decades, and the pinnacle of development here is 3DSTE (9-14). This technique has been an imaging tool available for nearly two decades, although it is still not widely used. The method combines the benefits of STE and 3D echocardiography, and in addition to volumetric measurements, it is capable of objectively characterizing LV contractility represented by LV strains and measuring spatial displacement of cardiac structures like valvular annuli as AAPSE (5,9-14). These LV strains may even characterize the spatial contraction

Table 3 Aortic valve plane systolic excursion and global left ventricular radial strain in different global left ventricular radial strain groups

Data	Global LV-RS ≤16.3% (n=15)	16.3% < global LV-RS <34.7% (n=83)	34.7% ≤ global LV-RS (n=13)	ANOVA P value
AAPSE (mm)	1.18±0.27	1.15±0.30	1.22±0.31	0.78
Basal LV-RS (%)	19.7±7.0	32.0±9.0†	50.8±11.4†‡	0.02
Midventricular LV-RS (%)	16.5±4.1	28.6±5.6†	50.8±8.5†‡	0.03
Apical LV-RS (%)	12.3±7.3	17.0±7.5†	27.8±12.2†‡	0.03
Global LV-RS (%)	13.0±3.1	24.9±4.8†	43.4±7.6†‡	0.02
Mean segmental LV-RS (%)	16.6±2.7	27.0±4.5†	45.1±7.9†‡	0.03
Basal LV-CS (%)	–24.5±4.7	–25.6±4.6	–30.2±5.1†‡	0.32
Midventricular LV-CS (%)	–27.4±4.8	–29.3±5.3	–34.1±6.7†‡	0.31
Apical LV-CS (%)	–29.0±8.8	–30.8±10.4	–32.8±13.1	0.88
Global LV-CS (%)	–25.7±4.4	–27.3±4.6	–31.3±5.8†‡	0.29
Mean segmental LV-CS (%)	–26.7±4.2	–28.3±4.4	–32.3±5.9†‡	0.32
Basal LV-LS (%)	–19.0±3.2	–20.5±4.5	–20.6±5.0	0.89
Midventricular LV-LS (%)	–12.2±3.1	–13.6±3.5	–13.6±4.0	0.87
Apical LV-LS (%)	–17.8±3.5	–17.1±5.3	–13.9±6.8†‡	0.35
Global LV-LS (%)	–15.2±1.5	–16.3±2.1†	–15.4±3.2	0.76
Mean segmental LV-LS (%)	–16.1±1.4	–17.1±2.0	–16.3±3.1	0.90

Data are presented as mean ± standard deviation. †, P<0.05 *vs.* global LV-RS ≤16.3%; ‡, P<0.05 *vs.* 16.3% < global LV-RS <34.7%. AAPSE, aortic valve annular plane systolic excursion; CS, circumferential strain; LS, longitudinal strain; LV, left ventricular; RS, radial strain.

pattern of a given LV region, which is known to have non-uniformity, meaning that certain LV regions participate to different degrees in shaping LV function (6-8). 3DSTE allows simultaneous assessment of global, regional and segmental unidimensional/unidirectional LV-LS, LV-CS and LV-RS using the same acquired 3D dataset together with volumetric assessments and AAPSE allowing very detailed functional analysis (5-7,9-14,16).

The AV is a key element of the aortic root having three thin semilunar leaflets and a fibrous AVA allowing one-way flow of the blood from the LV to the aorta (1,2). The AVA exhibits not only dimensional changes during the cardiac cycle but also spatial displacement represented by AAPSE due to the functional activity of adjacent muscular structures (5,17-19). AVA moves longitudinally during the cardiac cycle, i.e. towards the LV apex, and this is featured by the MME-derived AAPSE measured in cm. Therefore, the MME-based AAPSE is considered to be a characteristic of LV longitudinal function (3,4). However, 3DSTE can also be used for determination of AAPSE, which raises the possibility of an even more complex analysis of this phenomenon (5). Interestingly, the relationship between AAPSE with LV strains, objective features of LV contractility, which are widely used in clinics, has not been investigated so far, not even in healthy circumstances.

The present study has several implications. First of all, it can be stated that extensive LV functional analysis can be performed in a short time using 3DSTE, since in addition to all the LV strain measurements detailed above, AAPSE can also be measured simultaneously. This allows the analysis of the relationship between the two types of parameters, as done in this research. Second, the results of the study demonstrated that decreased AAPSE was associated with increased apical LV-LS. Interestingly, basal LV strains showed no associations with AAPSE. Moreover, increased AAPSE was associated with increased midventricular and apical (and global) LV-CS, but showed no associations with LV-RS and LV-LS. Third, global LV-RS, LV-CS and LV-LS showed no significant associations with AAPSE, but tended to be increased in the presence of larger- or smaller-than-average LV strains. It is important to realize that these findings were obtained in healthy individuals. The present

Table 4 Aortic valve plane systolic excursion and global left ventricular circumferential strain in different global left ventricular circumferential strain groups

Data	Global LV-CS ≤–22.6% (n=12)	–22.6% < global LV-CS <–32.6% (n=81)	–32.6% ≤ global LV-CS (n=18)	ANOVA P value
AAPSE (mm)	1.23±0.30	1.14±0.31	1.20±0.28	0.78
Basal LV-RS (%)	33.1±10.4	30.7±10.7	41.1±14.6‡	0.76
Midventricular LV-RS (%)	24.7±5.2	28.4±9.1	39.0±12.7†‡	0.74
Apical LV-RS (%)	12.0±5.5	16.5±7.8†	25.7±11.4†‡	0.12
Global LV-RS (%)	21.0±6.1	24.2±7.5	34.6±11.4†‡	0.87
Mean segmental LV-RS (%)	24.7±5.4	26.3±7.1	36.5±11.3†‡	0.21
Basal LV-CS (%)	–22.7±4.4	–25.2±4.2†	–31.8±4.2†‡	0.05
Midventricular LV-CS (%)	–23.1±4.0	–28.6±3.9†	–38.2±4.1†‡	0.05
Apical LV-CS (%)	–17.3±8.4	–30.3±8.6†	–40.9±9.4†‡	0.04
Global LV-CS (%)	–19.6±2.4	–26.8±2.7†	–35.8±2.4†‡	0.05
Mean segmental LV-CS (%)	–21.5±2.7	–27.7±2.7†	–36.5±2.5†‡	0.05
Basal LV-LS (%)	–21.0±3.2	–20.3±4.5	–19.9±4.7	0.89
Midventricular LV-LS (%)	–12.6±3.4	–13.1±3.6	15.0±3.2‡	0.65
Apical LV-LS (%)	–13.7±4.3	16.9±5.1†	18.4±6.7†	0.35
Global LV-LS (%)	–15.3±2.4	–16.0±2.1	–16.8±2.5	0.78
Mean segmental LV-LS (%)	–16.0±2.1	–16.8±2.0	–17.7±2.4	0.87

Data are presented as mean ± standard deviation. †, P<0.05 *vs.* global LV-CS ≤–22.6%; ‡, P<0.05 *vs.* –22.6% < global LV-CS <–32.6%. AAPSE, aortic valve annular plane systolic excursion; CS, circumferential strain; LS, longitudinal strain; LV, left ventricular; RS, radial strain.

analysis draws attention to a deeper and more complex association than it had been known so far. Results based on 3DSTE analysis could suggest that AAPSE seems to be more a 3D movement as was considered from MME analysis. Many internal and external factors, however, can influence this delicate balance. In addition to the classical and widely studied parameters, it is also worth considering factors such as the shape or deformity of the chest (like pectus excavatum), the effect of which on the examined parameters has been proven (20). An important question is how this balanced and sensitive relationship is disrupted in any other disease affecting the AV or the LV myocardium. Accordingly, further studies are needed to clarify this.

Limitation section

The following important limitations should be acknowledged:

- Although the study included apparently healthy individuals, it cannot be stated with 100% certainty that they were truly healthy, as additional exclusion tests would have been necessary.
- The image quality of 3DSTE is still less usable than that of 2D echocardiography. This can be explained by the lower temporal and spatial resolution, the size of the transducer, etc., which limits its applicability (9-14).
- This study did not consider the assessment of parameters with other imaging tests as part of the study.
- Moreover, the study did not aim to compare AAPSE with MME and 3DSTE, as well.
- 3DSTE is also suitable for many other evaluations, such as chamber quantifications and examination of the atrioventricular valvular annuli, but these analyses were not carried out in this study.
- Although the close relationship between the AVA and the aorta is known, investigating it was not the subject of the present study.
- The present study did not aim to determine the relationship between the dimensions of the AVA and LV strains, which could be a topic of future investigations.

Table 5 Aortic valve annular plane systolic excursion and global left ventricular longitudinal strain in different global left ventricular longitudinal strain groups

Data	Global LV-LS ≤–13.8% (n=19)	–13.8% < global LV-LS <–18.4% (n=76)	–18.4% ≤ global LV-LS (n=16)	ANOVA P value
AAPSE (mm)	1.16±0.30	1.15±0.29	1.19±0.35	0.88
Basal LV-RS (%)	33.4±12.3	31.8±11.6	35.1±12.8	0.86
Midventricular LV-RS (%)	32.0±12.3	28.9±9.8	29.9±11.4	0.76
Apical LV-RS (%)	18.1±11.5	17.1±8.3	19.9±9.4	0.81
Global LV-RS (%)	27.0±10.9	24.6±8.6	27.6±9.1	0.80
Mean segmental LV-RS (%)	29.1±10.6	27.0±8.0	29.3±8.9	0.76
Basal LV-CS (%)	–26.8±4.5	–25.7±5.0	–26.4±5.0	0.82
Midventricular LV-CS (%)	–29.2±5.5	–29.6±5.5	–30.3±6.9	0.91
Apical LV-CS (%)	–25.7±10.7	–30.6±9.6†	–37.7±11.0†‡	0.08
Global LV-CS (%)	–26.1±5.5	–27.5±4.4	–29.8±5.0†‡	0.07
Mean segmental LV-CS (%)	–27.4±4.9	–28.4±4.4	–30.7±5.7‡	0.25
Basal LV-LS (%)	–17.8±3.1	–20.2±4.0†	–23.7±5.3†‡	0.05
Midventricular LV-LS (%)	–10.9±3.6	–13.5±3.2†	–15.5±3.5†‡	0.05
Apical LV-LS (%)	–12.9±4.4	–16.8±4.6†	–22.1±5.9†‡	0.04
Global LV-LS (%)	–12.8±1.0	–16.1±1.3†	–19.6±0.9†‡	0.04
Mean segmental LV-LS (%)	–14.0±0.9	16.8±1.3†	–20.2±1.0†‡	0.05

Data are presented as mean ± standard deviation. †, P<0.05 *vs.* global LV-LS ≤–13.8%; ‡, P<0.05 *vs.* –13.8% < global LV-LS <–18.4%. AAPSE, aortic valve annular plane systolic excursion; CS, circumferential strain; LS, longitudinal strain; LV, left ventricular; RS, radial strain.

Table 6 Intra- and interobserver variability for three-dimensional speckle-tracking echocardiography-derived aortic valve annular systolic excursion and global left ventricular strains

Data	Intraobserver agreement			Interobserver agreement		
	Mean ± 2SD	ICC	P value	Mean ± 2SD	ICC	P value
Global LV-RS (%)	–0.8±1.6	0.85	<0.05	–0.9±1.8	0.81	<0.05
Global LV-CS (%)	–0.8±1.7	0.82	<0.05	–0.8±1.9	0.78	<0.05
Global LV-LS (%)	–0.9±2.0	0.82	<0.05	–1.0±2.1	0.79	<0.05
AAPSE (cm)	–0.03±0.15	0.92	<0.01	–0.03±0.21	0.92	<0.01

Intraobserver agreement: by 2 measurements of the same observer. Interobserver agreement: by 2 measurements of two independent observers. AAPSE, aortic valve annular plane systolic excursion; CS, circumferential strain; LS, longitudinal strain; LV, left ventricular; RS, radial strain; SD, standard deviation.

- ❖ During statistical analysis, only pairwise differences could be demonstrated without an overall effect, which increases the risk of Type I error and may mislead readers. This fact should be considered, when interpreting results.

Conclusions

There is a balanced and sensitive relationship between AAPSE and regional LV strains as assessed during the same 3DSTE in healthy adults.

Acknowledgments

None.

Footnote

Reporting Checklist: The authors have completed the STROBE reporting checklist. Available at https://qims.amegroups.com/article/view/10.21037/qims-2025-aw-2493/rc

Data Sharing Statement: Available at https://qims.amegroups.com/article/view/10.21037/qims-2025-aw-2493/dss

Funding: None.

Conflicts of Interest: All authors have completed the ICMJE uniform disclosure form (available at https://qims.amegroups.com/article/view/10.21037/qims-2025-aw-2493/coif). A.N. serves as an unpaid editorial board member of *Quantitative Imaging in Medicine and Surgery*. The other authors have no conflicts of interest to declare.

Ethical Statement: The authors are accountable for all aspects of the work in ensuring that questions related to the accuracy or integrity of any part of the work are appropriately investigated and resolved. This study was conducted in accordance with the Declaration of Helsinki and its subsequent amendments. The study was approved by the Institutional and Regional Human Biomedical Research Committee at the University of Szeged, Hungary (No. 71/2011, latest approval was given on 17th March, 2025). Written informed consent was given by all participants.

References

1. Loukas M, Bilinsky E, Bilinsky S, Blaak C, Tubbs RS, Anderson RH. The anatomy of the aortic root. Clin Anat 2014;27:748-56.
2. Anderson RH. Clinical anatomy of the aortic root. Heart 2000;84:670-3.
3. Jingi AM, Hamadou B, Noubiap JJ, Mfeukeu-Kuate L, Boombhi J, Nganou CN, Ateba NA, Ndoadoumgue AL, Nyaga UF, Menanga A, Kingue S. Correlations of left ventricular systolic function indices with aortic root systolic excursion (ARSE): A cross-sectional echocardiographic study. PLoS One 2018;13:e0206199.
4. Ünlüer EE, Karagöz A, Bayata S, Akoğlu H. An alternative approach to the bedside assessment of left ventricular systolic function in the emergency department: displacement of the aortic root. Acad Emerg Med 2013;20:367-73.
5. Nemes A, Ambrus N, Lengyel C. The Dimensions of the Aortic Valve Annulus Are Not Associated with Systolic Excursion of Its Plane in the Same Healthy Adults: Detailed Insights from the Three-Dimensional Speckle-Tracking Echocardiographic MAGYAR-Healthy Study. J Clin Med 2025;14:5760.
6. Kleijn SA, Brouwer WP, Aly MF, Rüssel IK, de Roest GJ, Beek AM, van Rossum AC, Kamp O. Comparison between three-dimensional speckle-tracking echocardiography and cardiac magnetic resonance imaging for quantification of left ventricular volumes and function. Eur Heart J Cardiovasc Imaging 2012;13:834-9.
7. Kleijn SA, Aly MF, Terwee CB, van Rossum AC, Kamp O. Reliability of left ventricular volumes and function measurements using three-dimensional speckle tracking echocardiography. Eur Heart J Cardiovasc Imaging 2012;13:159-68.
8. Narang A, Addetia K. An introduction to left ventricular strain. Curr Opin Cardiol 2018;33:455-63.
9. Franke A, Kuhl HP. Second-generation real-time 3D echocardiography: a revolutionary new technology.

MedicaMundi 2003;47:34.
10. Ammar KA, Paterick TE, Khandheria BK, Jan MF, Kramer C, Umland MM, Tercius AJ, Baratta L, Tajik AJ. Myocardial mechanics: understanding and applying three-dimensional speckle tracking echocardiography in clinical practice. Echocardiography 2012;29:861-72.
11. Urbano-Moral JA, Patel AR, Maron MS, Arias-Godinez JA, Pandian NG. Three-dimensional speckle-tracking echocardiography: methodological aspects and clinical potential. Echocardiography 2012;29:997-1010.
12. Muraru D, Niero A, Rodriguez-Zanella H, Cherata D, Badano L. Three-dimensional speckle-tracking echocardiography: benefits and limitations of integrating myocardial mechanics with three-dimensional imaging. Cardiovasc Diagn Ther 2018;8:101-17.
13. Gao L, Lin Y, Ji M, Wu W, Li H, Qian M, Zhang L, Xie M, Li Y. Clinical Utility of Three-Dimensional Speckle-Tracking Echocardiography in Heart Failure. J Clin Med 2022;11:6307.
14. Kleijn SA, Pandian NG, Thomas JD, Perez de Isla L, Kamp O, Zuber M, Nihoyannopoulos P, Forster T, Nesser HJ, Geibel A, Gorissen W, Zamorano JL. Normal reference values of left ventricular strain using three-dimensional speckle tracking echocardiography: results from a multicentre study. Eur Heart J Cardiovasc Imaging 2015;16:410-6.
15. Lang RM, Badano LP, Mor-Avi V, Afilalo J, Armstrong A, Ernande L, Flachskampf FA, Foster E, Goldstein SA, Kuznetsova T, Lancellotti P, Muraru D, Picard MH, Rietzschel ER, Rudski L, Spencer KT, Tsang W, Voigt JU. Recommendations for cardiac chamber quantification by echocardiography in adults: an update from the American Society of Echocardiography and the European Association of Cardiovascular Imaging. Eur Heart J Cardiovasc Imaging 2015;16:233-70.
16. Nemes A, Kormányos Á, Kalapos A, Domsik P, Gyenes N, Ambrus N, Lengyel C. Normal reference values of left ventricular strain parameters in healthy adults: Real-life experience from the single-center three-dimensional speckle-tracking echocardiographic MAGYAR-Healthy Study. J Clin Ultrasound 2021;49:368-77.
17. Baumgartner H, Falk V, Bax JJ, De Bonis M, Hamm C, Holm PJ, Iung B, Lancellotti P, Lansac E, Rodriguez Muñoz D, Rosenhek R, Sjögren J, Tornos Mas P, Vahanian A, Walther T, Wendler O, Windecker S, Zamorano JL; ESC Scientific Document Group. 2017 ESC/EACTS Guidelines for the management of valvular heart disease. Eur Heart J 2017;38:2739-91.
18. Silva RC, Mariani J Jr, Falcão BAA, Filho AE, Nomura CH, Avila LFR, Parga JR, Lemos Neto PA. Differences between systolic and diastolic dimensions of the aortic valve annulus in computed tomography angiography in patients undergoing percutaneous implantation of aortic valve prosthesis by catheter. Rev Bras Cardiol Invasiva 2015;23:130-3.
19. Nemes A, Ambrus N, Lengyel C. Normal reference values of three-dimensional speckle-tracking echocardiography-derived aortic valve annular dimensions in healthy adults-a detailed analysis from the MAGYAR-Healthy Study. Quant Imaging Med Surg 2025;15:6776-86.
20. Sonaglioni A, Nicolosi GL, Trevisan R, Lombardo M, Grasso E, Gensini GF, Ambrosio G. The influence of pectus excavatum on cardiac kinetics and function in otherwise healthy individuals: A systematic review. Int J Cardiol 2023;381:135-44.

Cite this article as: Nemes A, Ambrus N, Lengyel C. How aortic valve annular plane systolic excursion and left ventricular strains are associated in healthy adults measured simultaneously by three-dimensional speckle-tracking echocardiography? (Insights from MAGYAR-Healthy Study). Quant Imaging Med Surg 2026;16(4):306. doi: 10.21037/qims-2025-aw-2493